MAUSAM, **77**, 1 (January, 2026), 83-98

MAUSAM

DOI: https://doi.org/10.54302/whzrqr25
Homepage: https://mausamjournal.imd.gov.in/index.php/MAUSAM

UDC No.551.553.21:551.509.3(540)

# Evaluation of seasonal prediction skills of summer monsoon precipitation over Pan India

LATA VISHNOI[1*], RSK MAURYA[4], DR PATTANAIK[1], ANUPAM KUMAR[2],
KK SINGH[3] SC BHAN[1] and PRIYANKA SINGH[1]

[1]*India Meteorological Department, New Delhi,*

[2]*Nanyang Technological University, Singapore*

[3]*Association of Agrometeorologists, Anand Agricultural University, Gujarat, India*

[4]*Indian Institute of Tropical Meteorology, Pune, India,*

(*Received 29 January 2024, Accepted 25 February 2025*)

***Corresponding author's email: lata.vishnoi@gmail.com**

**सार** – दक्षिण-पश्चिम (SW) मॉनसून का मौसम (जून, जुलाई, अगस्त और सितंबर) भारत में वर्षा की मुख्य अवधि है। यह अध्ययन मुख्य रूप से तीन अलग-अलग सांख्यिकीय तरीकों, जैसे "सिंगुलर वैल्यू डीकंपोजिशन-आधारित मल्टीपल रिग्रेशन", "सुपरवाइज्ड प्रिंसिपल कंपोनेंट रिग्रेशन" और "कैनोनिकल कोरिलेशन विश्लेषण" का उपयोग करके कई जनरल सर्कुलेशन मॉडल (GCMs) के आउटपुट का उपयोग करके SW मॉनसून की भविष्यवाणी से संबंधित था। वर्तमान अध्ययन में, मल्टी-मॉडल एन्सेम्बल (MME) दृष्टिकोण का मूल्यांकन जनरल सर्कुलेशन मॉडल (GCMs) के परिणामों के आधार पर किया गया था। भारत के 34 मौसम विज्ञान उप-मंडलों में अप्रैल और मई महीने की शुरुआती स्थितियों के साथ ग्रीष्मकालीन मॉनसून2020 और 2021 के लिए ERFS परियोजना के तहत अपरिष्कृत संकल्पMME-GCMs से मॉडल आउटपुट के रूप में वर्षा पूर्वानुमान उत्पन्न किया गया था। MME-GCMs आधारित वर्षा आउटपुट के प्रदर्शन का मूल्यांकन 1982 से 2019 की अवधि के लिए भा. मौ. वि. वि.द्वारा देखी गई वर्षा के मुकाबले किया गया था। सिम्युलेटेड GCMs वर्षा का मूल्यांकन विभिन्न सांख्यिकीय विश्लेषणों जैसे जलवायु औसत, मानक विचलन, मानकीकृत विसंगति सूचकांक, पूर्वानुमान पूर्वाग्रह, रूट मीन स्क्वायर त्रुटि (RMSE), सहसंबंध गुणांक, और चरण सुसंगतता सूचकांक आदि के साथ किया गया था। यह देखा गया कि वर्षा के स्थानिक प्रतिरूप को अच्छी तरह से कैप्चर और प्रस्तुत किया गया था। अधिकांश MME-GCMs मध्य भारत और पश्चिमी घाटों पर वर्षा के वितरण को कम आंकते हैं, जबकि प्रायद्वीपीय भारत में इसे अधिक आंकते हैं। प्रत्येक क्षेत्र के लिए अलग-अलग MME-GCMs द्वारा स्थानिक और लौकिक सहसंबंध गुणांकों को अच्छी तरह से कैप्चर किया गया था। ERFS आधारित भविष्यवाणी का सत्यापन ग्रीष्मकालीन मॉनसून के मौसम के लिए किया गया था। भारत के 34 मौसम विज्ञान उप-मंडलों में 3∗3 आकस्मिकता तालिका का उपयोग करके पूर्वानुमान सटीकता (ACC), पूर्वाग्रह स्कोर (BIAS), पता लगाने की संभावना (POD), मिथ्या अलार्म दर (FAR) और जोखिम स्कोर (TS) जैसे कौशल स्कोर की गणना की गई थी। पूरे देश के लिए, 2020 और 2021 में देखी गई (IMD) मौसमी ग्रीष्मकालीन मॉनसून वर्षा क्रमशः लंबी अवधि के औसत (LPA) का 109% और 99% थी। अप्रैल और मई के लिए दो अलग-अलग शुरुआती स्थितियों का उपयोग करके ERF से वर्षा का पूर्वानुमान 2020 के गर्मी के मॉनसून में LPA का 107% और 112% था और 2021 के गर्मी के मॉनसून में LPA का 105% और 102% था। वर्षा का पूर्वानुमान मेट-सब-डिवीजन स्तर पर बेहतर दिखाया गया, यानी 2020 के मॉनसून के दौरान 0.53 और 0.59 और 2021 के मॉनसून के दौरान अप्रैल और मई की शुरुआती स्थितियों के लिए क्रमशः 0.44 और 0.62।

**ABSTRACT.** The Southwest (SW) monsoon season (June, July, August, and September) is the major period of rainfall activity in India. This study was mainly concerned with the prediction of the SW monsoon using output of several General Circulation Models (GCMs) with three different statistical approaches, namely, singular value decomposition-based multiple regression, supervised principal component regression and canonical correlation analysis. In the present

study, the Multi-Model Ensemble (MME) approach was evaluated based on the results of General Circulation Models (GCMs). Precipitation forecast was generated as model output from coarse resolution MME-GCMs under ERFS project for summer monsoon 2020 and 2021 with April and May month's initial conditions over 34 meteorological sub-divisions of India. The performance of the MME-GCMs based precipitation outputs was evaluated against IMD observed precipitation for the period 1982 to 2019. The evaluation of simulated GCMs precipitation was done with various statistical analysis like climatological mean, standard deviation, standardized anomaly index, forecast bias, root mean square error (RMSE), correlation coefficients, and phase coherency index *etc*. It was observed that the spatial pattern of precipitation was well captured and presented. Most MME-GCMs underestimates the distribution of precipitation over central India and the Western Ghats, while overestimates in the peninsular India. The spatial and temporal correlation coefficients were well captured by the different MME-GCMs for each region. The verification of ERFS based prediction was done for the summer monsoon season. The skill scores like Forecast accuracy (ACC), bias score (BIAS), detection probability (POD), false alarm rate (FAR) and threat score (TS) were calculated using 3*3 contingency table over 34 meteorological sub-divisions of India. For the country as a whole, the observed (IMD) seasonal summer monsoon precipitation in 2020 and 2021 was 109% and 99% of the long-period average (LPA), respectively. The rainfall forecast from ERF using two different initial conditions for April and May, were 107% and 112% of the LPA in the 2020 summer monsoon and 105% and 102% of the LPA in the 2021 summer monsoon. The precipitation forecast was better represented at metsub-division level *i.e.* 0.53 and 0.59 during the 2020 monsoon and 0.44 and 0.62 during the 2021 monsoon for the April and May initial conditions, respectively.

**Key words** – Summer monsoon, GCM, ERF, Forecast verification and MME.

## 1. Introduction

Approximately 80% of the annual rainfall over the Indian subcontinent occurs during the Indian Summer Monsoon Period (ISMP), which spans from June to September. This four-month period, often referred to by the abbreviation JJAS (June, July, August, September), consists of 122 days and is characterized by the dominant monsoon season (Parthasarathy *et al*., 1994). The summer monsoon over India is associated with the complex structural system of the land-ocean-atmosphere phenomenon. Therefore, it was very difficult to predict the rainfall of the Indian summer monsoon over India. The characteristics of Indian summer monsoon precipitation are associated with mesoscale convective activities, intraseasonal variations, *etc*. (Koteswaram and Rao, 1963; Meehl *et al.,* 1993; Kripalani *et al*,. 2003; Krishnamurti *et al*., 2010; Niyogi *et al*., 2010; Mohanty *et al*., 2019b). A seasonal prediction using a dynamical multi-model technique has predicted the average weather states at any region for advanced information. Multimodel ensemble (MME) forecast method have delivered a convincing capacity to improve forecast in wider regions as computational approaches The use of mathematical equations has solved the dynamical and physical processes ultimately of the atmosphere variables in the modeling framework for forthcoming time steps (Abbe, 1901; Richardson, 1922; Phillips, 1956; Smagorinsky, 1963). Advanced dynamical models, such as atmospheric models (Pattanaik and Kumar, 2010), coupled ocean-atmosphere models (Saji *et al.,* 1999; Webster *et al.,* 1999; Ashok *et al.,* 2004) and coupled land–atmosphere models are used for improved seasonal prediction.

General circulation models (GCMs) are integrated with various forecast related systems to deliver monthly and seasonal forecasts across the globe. The skills of several studied comparisons of simulated GCM precipitation have improved quite well (Gadgil and Sajani, 1998; Krishnamurti *et al.,* 2000; Palmer *et al.,* 2004; Rajeevan and Nanjundiah, 2009; Kar *et al*., 2011; Sperber *et al.,* 2012; Sabeerali *et al*., 2013; Pillai *et al.,* 2018). Several GCM products have improved the prediction skill of the ISMP in India (Webster *et al.,* 1999; Simmons and Hollingsworth, 2002; Gadgil and Srinivasan, 2011; Nair *et al.,* 2015). The improvement in the forecast skill of the various GCM models has considered the physical processes, data acquisition, data assimilation, ensemble prediction techniques and computation of high-performance models to help in operational seasonal forecasting (Kirtman *et al.,* 2014). The experimental forecast system created for the North American Multi Model Ensemble (NAMME) has supported intraseasonal, seasonal and interannual forecasts of the real-time MME since August 2011. There are ample indications of dynamic sub seasonal forecasts which are of acceptable quality, so it is reasonable to expect that multimodel approaches will improve the quality of forecasting (Palmer *et al.,* 2004; Hagedorn *et al.,* 2005; Doblas-Reyes *et al.,* 2005; Berner *et al*., 2008; Palmer *et al.,* 2008; Pegion and Sardeshmukh, 2011).

The International Research Institute for Climate and Society (IRI) provide MME techniques in collaboration with National Oceanic and Atmospheric Administration (NOAA), National Science Foundation (NSF), National Aeronautics and Space Administration (NASA), U.S. Department of Energy (DOE) and Asia Pacific Economic Cooperation (APEC) Climate Center (APCC), Korea. The IRI utilizes the MME techniques based on atmospheric and atmosphere-ocean GCMs (AGCMs and AOGCMs). The performance of the MME predictions has been evaluated with a significant reduction error, and it has improved the predictive capability (Kirtman and Min, 2009). The limitations of multimodel ensemble forecasts arise from the uncertainty of computational errors, initial

conditions, and the nonlinearity of the atmospheric process.

The Climate Forecast System Version 2 (CFSv2) was developed by the National Centres for Environmental Prediction (NCEP) and it has the potential to provide forecasts for the sub-seasonal to seasonal scale (Saha *et al*., 2014). The India Meteorological Department uses CFSv2 for skillful prediction of Indian summer monsoon (Chaudhari *et al.,* 2013; Saha *et al.,* 2014). The coupled anomaly model NCAR-COLA was developed by the National Centre for Atmospheric Research (NCAR), Centre for Ocean-Land-Atmosphere Studies (COLA) which successfully predicts the El Niño Southern Oscillation (ENSO; Kirtman, 2003; Tippett *et al.,* 2019). The Geophysical Fluid Dynamics Laboratory (GFDL) is supported by the Earth System Grid Federation USA at various resolutions of the GCMs product, adds carbon system models and enhanced ocean dynamics. The Environment and Climate Change Canada (ECCC) is the first organization to develop a dynamic seasonal forecasting system, which was based on the Historical Forecasting Project (Derome *et al*., 2001; Kharin *et al*., 2009). The ECCC consists of the Atmospheric General Circulation Model (Scinocca *et al.,* 2008) and the Global Spectral Model (Ritchie, 1991; Cote *et al.,* 1998), which were used to develop an ensemble seasonal prediction.

The experimental real-time extended range forecast system (ERFS) was developed by a dynamical-statistical technique using MME approach for predicting the monthly and seasonal precipitation and temperature (average, minimum and maximum) at the 34 meteorological subdivisions of India (Mohanty *et al*., 2018). This study builds on Mohanty *et al*. (2019a) by employing advanced statistical techniques, such as Singular Value Decomposition, Supervised Principal Component Regression, and Canonical Correlation Analysis, to improve the evaluation of seasonal precipitation predictions at a regional scale. Compared to Mohanty *et al*. (2019b), this work utilizes updated global model outputs, enhancing operational predictability and more effectively capturing interannual variability for the Indian summer monsoon. The dynamical approach is based on the nesting of GCMs to simulate high-resolution regional-scale consistent physical processes with large-scale weather evaluation. The statistical approach is based on the statistical relationships between the regional climate and the statistical characteristics of the desired fields assumed from the coarse-resolution GCM data. Within the statistical approach, the performance of the different AGCM/AOGCM outputs obtained from different lead time scales were evaluated using appropriate bias corrections. The appropriate bias-corrected GCM results were combined with different statistical techniques, such as a simple mean, a multivariate regression technique based on the singular value decomposition method, supervised principal component regression (sup-PCR) and canonical correlation analysis (CCA). The methods like combined simple ensemble mean (Doblas-Reyes *et al.,* 2000; Pavan and Doblas-Reyes, 2000; Stephenson and Doblas-Reyes, 2000; Peng *et al*., 2002; Palmer *et al.,* 2004), the regression-improved ensemble mean (Peng *et al.,* 2002; Kharin and Zwiers, 2003), bias-removed ensemble mean (Kharin and Zwiers, 2002) and multi model ensemble mean were included in the analysis (Krishnamurti *et al*., 2000a, b. The combined predictions of the MME showed higher prediction skills as compared to the individual member models (Krishnamurti *et al.,* 2000 a, b; Yun *et al.,* 2003, 2005).

The examination of the real-time ERFS generated forecast products was verified during ISMP for the year 2020 and 2021, with two lead times between April and May initial conditions (ICs) over the 34 MSDs. The GCM simulated precipitation was evaluated against IMD's observed gridded data during the summer monsoon season of 1982-2019. The potential of MME models to capture mean seasonal features and predictability of the ISMP was also explored during the analysis. The prediction abilities of MME models can be expected to improve with prospective research by utilizing statistical/dynamical downscaling at the regional scale. The outcome of this analysis would provide a piece of valuable information on the ERFS forecast product certainty to decision-makers like the agriculture sector, water management, and hydropower sector, climate risk and research community *etc*.

## 2. Data and methodology

Brief detail about the North American multi-model ensemble (NMME) model products is described in this section as well as the development of the ERFS methodology.

### 2.1. *Brief detail about the NMME products and observations*

The eight GCM coupled models used in the present study, their model resolution, the number of ensemble members, product types, the number of forecast leads (in months) and references are listed in Table 1. CFSv2 is a fully coupled model in which interactions occur between the Earth's atmosphere, oceans, and land (Saha *et al.,* 2014) with 24 ensemble members. Each initial condition is made by one ensemble member, and they are initialized four times a day and six times a month. The CFSv2 has a spectral triangular truncation of T126 horizontal resolution (equivalent to 100 km grid resolution at the

**TABLE 1**

**Brief details of the GCMs used in this study**

| Sr. No. | Model | Resolution | Ensemble members | Type | References |
|---|---|---|---|---|---|
| 1 | CFS v2 (CFSV2) | T126 | 24 | Fully coupled | Saha *et al*. (2014) |
| 2 | GFDL-CM2p1-aer04 (GFDLA04) | T42 | 10 | Fully coupled | Kirtman *et al*. (2014) |
| 3 | GFDL-CM2p5-FLOR-A06 (GFDLA06) | T42 | 12 | Fully coupled | Kirtman *et al.* (2014) |
| 4 | GFDL-CM2p5-FLOR-B01 (GFDLB01) | T42 | 12 | Fully coupled | Kirtman *et al.* (2014) |
| 5 | COLA-RSMAS-CCSM4 (COLA) | T106 | 10 | Anomaly Coupled | Kirtman *et al.* (2014) |
| 6 | CanCM4i | T63 | 10 | Fully coupled | Merryfield *et al.* (2013) |
| 7 | CanSIPSv2 | T63 | 20 | Fully coupled | Merryfield *et al.* (2013) |
| 8 | GEM-NEMO | T85 | 10 | Fully coupled | Smith *et al.* (2013, 2018) |

equator) with 64 vertical sigma-pressure hybrid layers. The three different versions of the GFDL model are considered fully coupled models with different ocean resolutions at T42 horizontal resolution, such as GFDL-CM2p1-aer04 (GFDLA04; 10 ensemble members), GFDL-CM2p5-FLOR-A06 (GFDLA06; 12 ensemble members), and GFDL-CM2p5-FLOR-B01 (GFDLB01; 12 ensemble members), for a 12-month forecast. The COLA4 (COLA-RSMAS-CCSM4) is an Anomaly Coupled model. University of Miami (RSMAS) supported the Community Climate System Model version 4.0 (CCSM4) of the NCAR with 10 ensemble members has T106 horizontal resolution (equivalent 125 Km grid resolution at the equator) for 12 months prediction. The CCMEP of ECCC is based on a multimodel approach for developing a fully coupled operational model of the Canadian Centre for Climate Modelling and Analysis (CCCma) Coupled Climate Model version 4 (CanCM4) with Arctic sea ice thickness initial conditions (CanCM4i; Merryfield *et al.*, 2013), the Global Environmental Multiscale, the Nucleus for European Modelling of the Ocean (GEM-NEMO; Smith *et al*., 2013, 2018) and the Canadian Seasonal to Interannual Prediction System (CanSIPSv2; Merryfield *et al.,* 2013) with integrated 12 months for each model. CanCM4i has integrated 10 ensemble members at T63 horizontal resolution (equivalent to 210 km grid resolution at the equator), with 35 vertical levels and 1 hPa at the top. GEM-NEMO has a horizontal resolution of a 256 × 128 Gaussian grid (T85) with 79 vertical levels and 0.075 hPa at the top with 10 ensemble members. CanSIPSv2 involves a multimodel ensemble system with two coupled atmosphere-ocean models, CanCM4i and GEM-NEMO, with 20 ensemble members.

The eight GCMs simulated precipitation were compared for April and May ICs during the ISMP for the period of 1982-2019 (38 years) over the Indian subcontinent. GCM ensemble members were considered for average seasonal prediction as well as inter comparison for Indian conditions (Johnson *et al.,* 2017; Trenary *et al.,* 2017; Pillai *et al.,* 2021). IMD daily gridded precipitation (spatial resolution at 0.25°×0.25°; Pai *et al.,* 2014) was used for the performance of the GCMs. The spatial analysis of the eight GCMs simulated precipitation for April and May ICs used different statistical techniques, such as climatological mean, standard deviation, standardized anomaly index, forecast bias, root mean square error (RMSE), correlation coefficients and phase coherency index.

### 2.2. *Experimental real-time ERFS precipitation forecast*

MME techniques were used to generate ERFS forecasts, such as simple mean ensembles, multiple linear regressions using singular value decomposition, supervised principal component regression (Sup-PCR) and canonical correlation analysis (CCA). The simple mean ensemble was normalized with their climatological mean later Standard Deviation (SD) was multiplied by the observed interannual variation and added to the observed climatology to obtain the final forecast (Hagedorn *et al.,* 2005). The multiple linear regression using the singular value decomposition method was taken as a weighted MME mean. The use of multiple linear regression techniques has been utilized in singular value decomposition (Krishnamurti *et al.,* 2000a, b; Yun *et al.,* 2003). The Sup-PCA method was implemented in two stages. In the first stage, the predictor was filtered by the threshold value of the correlation between the predictor (model) and predictand (observed). In the second stage, the use of the rank of PCA was based on the correlation between observations and the model. Eventually, PCA founded on its rank is added sequentially to the regression equation and considered the minimum root mean square error for a threshold correlation of that model (Fekedulegn *et al.,* 2002; Acharya *et al.,* 2012; Nair *et al.,* 2012; Nageswararao *et al.,* 2016c). The CCA methods were

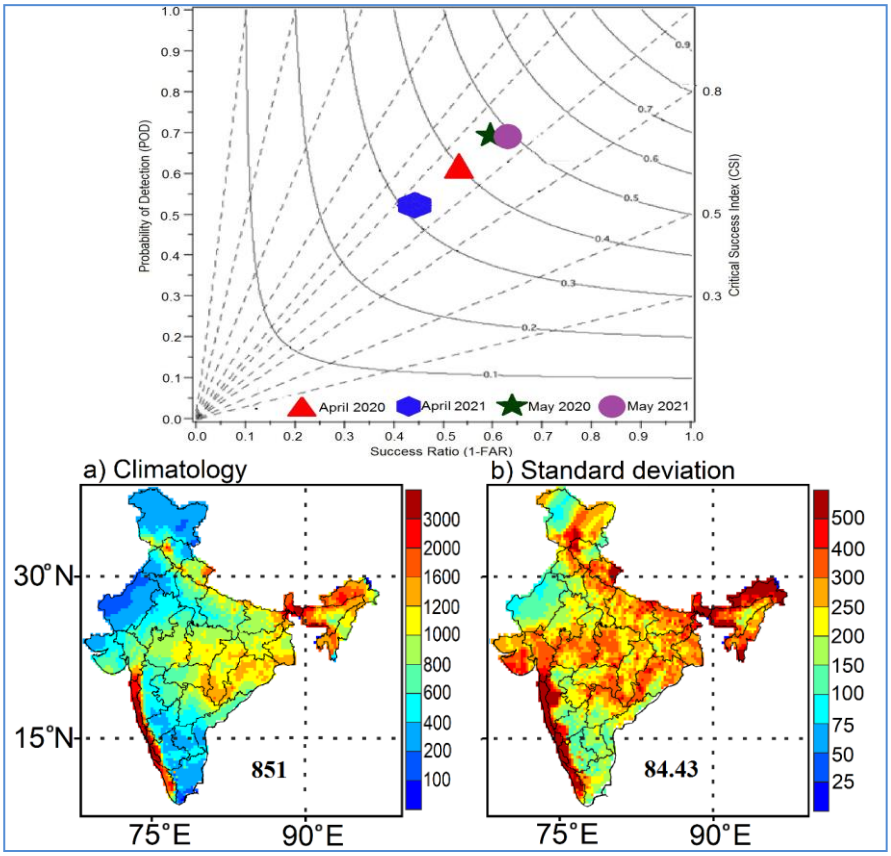


**Figs. 1(a&b).** Spatial distribution of the summer monsoon season precipitation (mm) obtained by the IMD for the period 1982 to 2019: a) climatology and b) standard deviation (Sd)

established empirical orthogonal functions (EOFs), and matrix correlation between predictor and predictand was added (Wilks, 1995; Barnston and Smith 1996; Yu *et al.*, 1997; Sinha *et al.*, 2013).

Verification of the ERFS deterministic precipitation forecast is usually arranged in a 3×3 contingency table, as shown in Table 2, belonging to the three precipitation departures categorized as deficit (-20% or less), normal (-19% to 19%), and excess (20% or more) at 34 MSD. The multicategory of the contingency table was carried out for four standards categories to belongs to “Hits”, “Misses”, “False Alarms”, and “Correct Negatives” that found of the frequency "yes" and "no" occurrences of forecast. The quantitative forecast precipitation verifying method was used for Yes/No events (Brier and Allen, 1951; Murphy *et al.*, 1989; Murphy and Winkler, 1992; Wilks, 1995) for different forecast skill scores (Table 3). The forecast accuracy (ACC) is the ratio of correct predictions over the total number of events. The bias score (BIAS) is the ratio of the frequency of forecast events to the frequency of observed events (Fowler *et al.*, 2012). A perfect forecast is indicated by no bias, less than one is under forecast, and more than one is over forecast (Wilks, 2011). The probability of detection (POD) is the ratio of the correct events to the observed events, also understood as the hit rate while ignoring false alarms. The false alarm ratio (FAR) is the ratio of false events to forecast events, with zero representing a perfect forecast. The critical success index (CSI) is known as the threat score. The correct negative events are not considered, and the forecast events are evaluated relative to the observed events. The success ratio (SR) is the ratio of the hits to the forecast events but ignores misses.

## 3. Results and discussion

### 3.1. *Distribution of the observed and GCM precipitation*

The high-resolution gridded daily precipitation data provided by the IMD were spatially distributed, and the mean climatology and standard deviation of the summer monsoon season from 1982-2019 over India was presented in Figs. 1 (a & b). The spatial distribution of mean JJAS precipitation (Fig. 1a) was highest in the Western Ghats (WGs), North-East India (NEI), and Central India (CI), while the lowest distribution was in

**TABLE 2**

**Contingency table (3×3) for the deterministic forecast**

| | | Observed | | |
|---|---|---|---|---|
| | | **Excess** | **Normal** | **Deficit** |
| Forecast | **Excess** | Hits | Misses | False Alarms |
| | **Normal** | Misses | Hits | False Alarms |
| | **Deficit** | False Alarms | Misses | Correct Negatives |
| Excess (20% or more); | | Normal (-19% to 19%); | | Deficit (-20% or less) |

**Table 3**

**Methods for forecast verification**

| Sr.No. | Skill | Formula | Range | Characteristics |
|---|---|---|---|---|
| **1** | Accuracy (ACC) | $\frac{\text{Hits + Corret Negatives}}{\text{Total}}$ | 0 to 1 | Perfect: 1 |
| **2** | Bias score (BIAS) | $\frac{\text{Hits + False Alarms}}{\text{Hits + Misses}}$ | 0 to ∞ | Under forecast (BIAS<1) Over forecast (BIAS>1) |
| **3** | Probability of detection (POD) | $\frac{\text{Hits}}{\text{Hits + Misses}}$ | 0 to 1 | Perfect: 1 |
| **4** | False alarm ratio (FAR) | $\frac{\text{False Alarms}}{\text{Hits + False Alarms}}$ | 0 to 1 | Perfect: 0 |
| **5** | Critical success index (CSI) | $\frac{\text{Hits}}{\text{Hits + Misses + False Alarms}}$ | 0 to 1 | Perfect: 1 |
| **6** | Success ratio (SR) | $\frac{\text{Hits}}{\text{Hits + False Alarms}}$ | 0 to 1 | Perfect: 1; SR=1-FAR |
| **7** | Miss ratio (SR) | $\frac{\text{Misses}}{\text{Hits + Misses}}$ | 0 to 1 | Perfect: 1; SR=1-POD |

was in North-West India (NWI) and Interior Peninsular India (IPI). The maximum distribution of the mean JJAS precipitation over the WGs and NEI is the favoured location of the tropical convergence zone during the summer monsoon season. The average climatological precipitation for the whole country during the summer monsoon season of 1982-2019 (38 years) is approximately 851 mm. The spatial distribution of the SD (Fig. 1b) for the summer monsoon season of 1982-2019 was maximum, which has a high precipitation zone and vice versa. The standard deviation of the precipitation over India was approximately 84.43 mm for the period JJAS, 1982-2019. The climatological mean of the JJAS precipitation was eight GCM simulations for two initial conditions over India for a 38-years period is illustrated in Fig.2. The pattern distribution of the simulated JJAS precipitation was well captured in CFSv2, GFDLA04, GFDLA06 and COLA for the April and May ICs. The intensities of the simulated GCM JJAS precipitation were less than those of the observation (IMD), except for the COLA model for April and May ICs. The pattern intensities of the simulated GCM JJAS precipitation increased from April to May ICs. The three Canadian models, CanCM4i, CanSIPv2 and GEN-NEMO did not capture the pattern mean JJAS simulated precipitation well for both ICs. The mean pattern of JJAS simulated precipitation intensity was underestimated in most of the GCMs with both ICs. Most of the GCMs' simulated precipitation was underestimated during the summer monsoon season (Sabeerali *et al.*, 2013; Acharya *et al.*, 2014). The spatial pattern of the SD of eight GCM models was exhibited throughout India for the summer monsoon season of 1982-2019, with April and May ICs shown in Fig. 3. All the CGMs simulated JJAS precipitation with less standard deviation than that of the observation. The CFSv2, GFDLA06, GFDLB01, and COLA have shown a close SD pattern from the IMD with both ICs in April and May. The GFDLA06 and GFDLB01 SDs were highly increased from April to May ICs. Al the Canadian models did not capture the SD patterns well, where the deviation ranged from 35-39 mm with both ICs.

The Standardized Anomaly Index (SAI) was calculated by the frequency distribution (year-to-year fluctuations) for the mean JJAS precipitation for the period 1982-2019 over India, as presented in Fig.4. According to Edwards and McKee (1997), the SAI is computed by dividing the precipitation anomalies by the standard deviation, which gives the cumulative probability from a normal distribution. The frequency of dry and rainy years revealed the SAI of precipitation (Agnew and

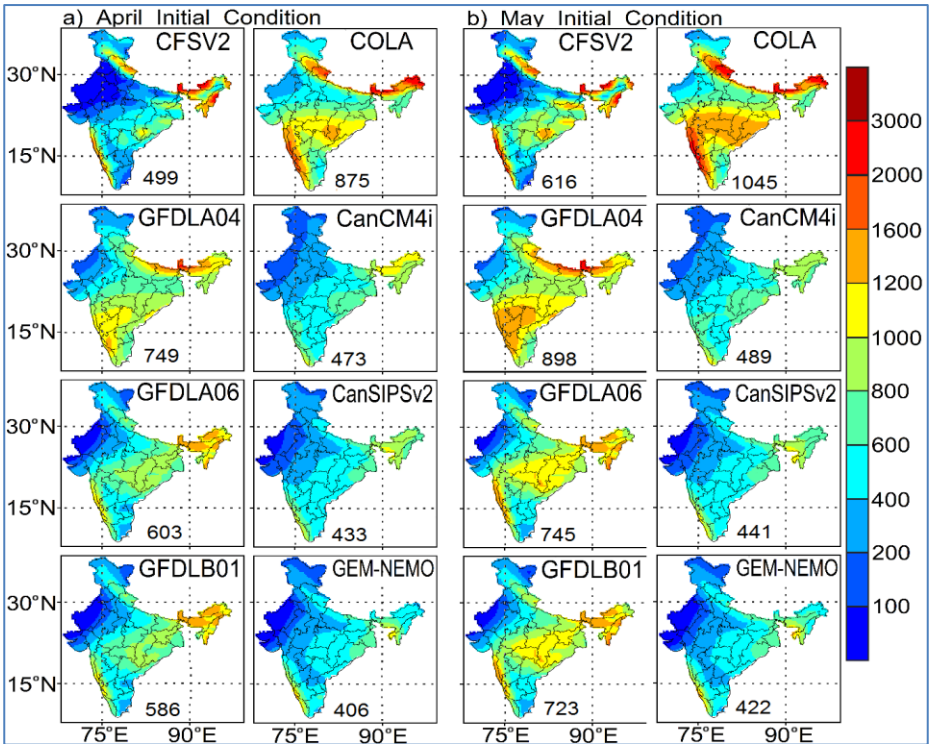


**Figs. 2(a&b).** Spatial distribution of the mean simulated precipitation (mm) during the summer monsoon season for the period 1982 to 2019: a) April initial condition and b) May initial condition. Eight global climate model (GCM) products are obtained by CFSV2, GFDLA04, GFDLA06, GFDLB01, COLA, CanCM4i, CanSIPSv2 and GEM-NEMO

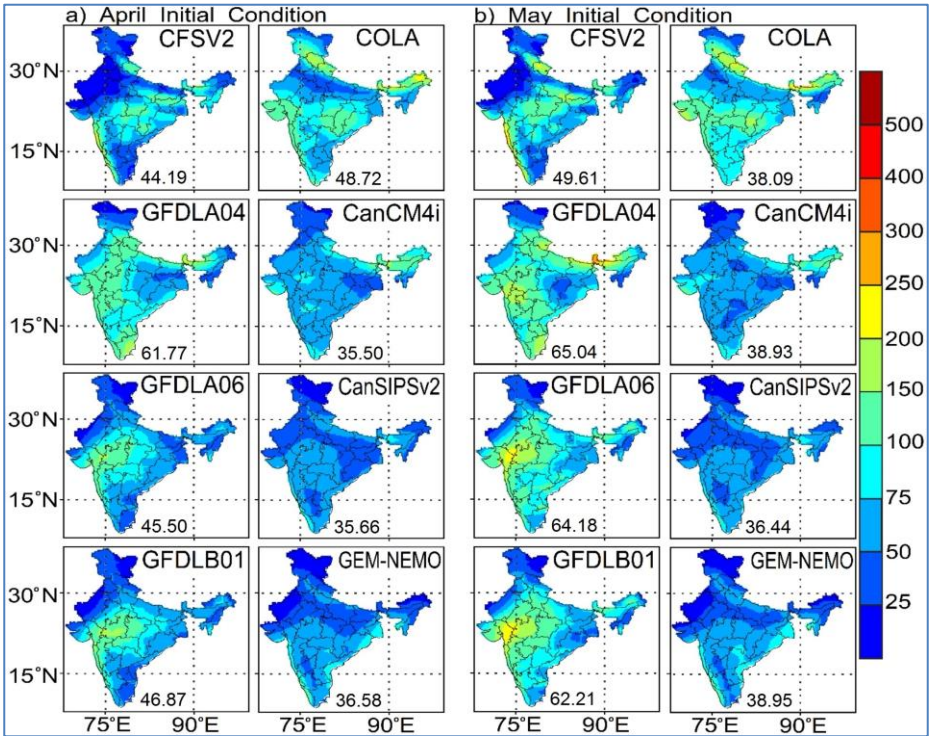


**Figs. 3(a&b).** Spatial distribution of SD for precipitation (mm) during the summer monsoon season for the period 1982-2019: a) April initial condition and b) May initial condition

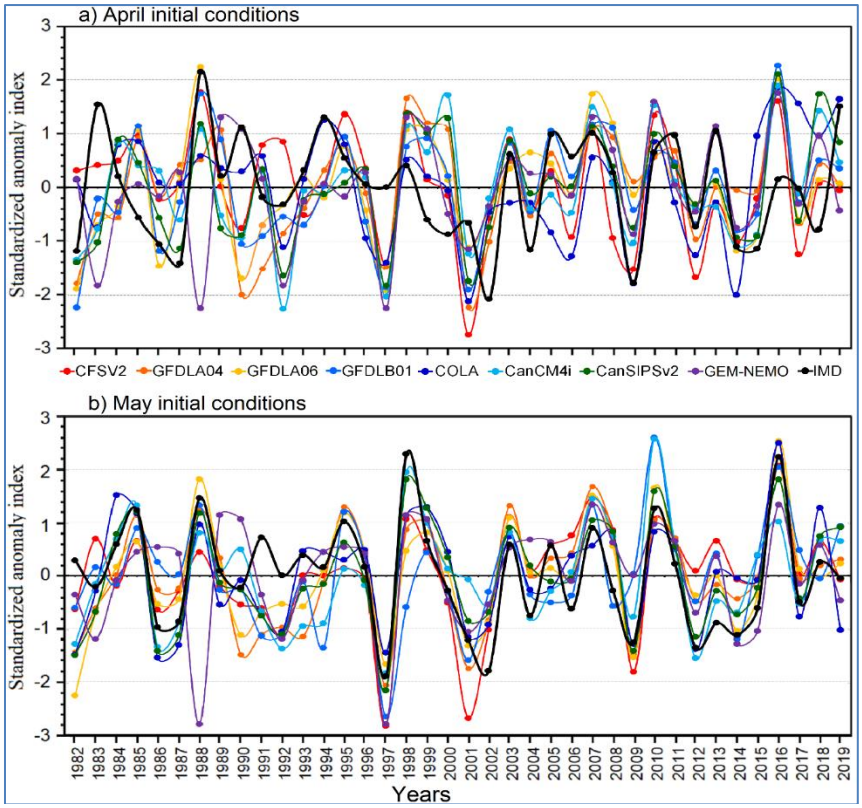


**Figs. 4(a&b).** Time series of the standardized anomaly index of eight GCM simulations and observed (IMD) precipitation over all Indian areal means during the summer monsoon season for the period 1982-2019: a) April initial condition and b) May initial condition

Chappel, 1999; Bewket and Conway, 2007). The precipitation from the eight GCM simulations and the IMD observation is shown in Fig. 4 (a & b), which show the SAI of the April and May ICs. The normalized time series of the JJAS precipitation varied year-to-year and were in very close agreement with the GCM simulation with observations for May ICs (lead-1) as compared to April ICs (lead-2). While the comparable sign (SAI) from IMD precipitation for the April ICs (total simulated 38 years) was matched of 22-25 years in COLA, GFDLA04, CanCM4i, and GFDLA06, it was a high match of 26-29 years in CFSv2, GFDLA06, GFDLB01, CanSIPv2, and GEN-NEMO. In CFSv2, GFDLA06, GFDLB01, CanCM4i, and GEN-NEMO, an increase in SAI in the May ICs had a similar indication of 28-31 years, whereas it ranged from 22-27 years in COLA, GFDLA04, and CanSIPv2. The SAI was matched for 22-27 years in COLA, GFDLA04, CanSIPv2, and GFDLA06, while the high match was 28-31 years in CFSv2, GFDLA06, GFDLB01, CanCM4i, and GEN-NEMO. The anomaly index of IMD for both ICs showed the lowest agreement between COLA and GFDLA04. The GCMs with IMD anomalies for April ICs were not obtained in the summer monsoon seasons of 1983, 1990, 1997, 1999, 2000, 2016, and 2018; similarly, the May ICs were not captured in the summer monsoon seasons of 1983, 1997, and 2016. The summer monsoon during strong El Niño periods has not been captured by the majority of the simulated GCM precipitation (Slingo and Annamalai, 2000).

### 3.2. *Standard errors of the GCM precipitation*

The spatial mean precipitation bias (forecast minus actual) computed for the GCMs simulated with IMD observations during JJAS 1982-2019 for April and May ICs is presented in Fig. 5. With the exception of COLA4, most of the simulated GCM precipitation was less than expected. The CFSv2, CanCM4i, CanSIPSv2, and GEN-NEMO have maxima underpredicted in the WGs, central India, and NEI, whereas maxima overpredicted precipitation were the COLA and GFDLA04 over peninsular India for April and May ICs. The simulated GCM precipitation was increased in each GCM for April to May ICs, but the maximum increase was in CFSv2, GFDLA04, GFDLA06, GFDLB01, and COLA. The WGs for both ICs show the highest negative bias of all simulated GCM precipitation. Due to its

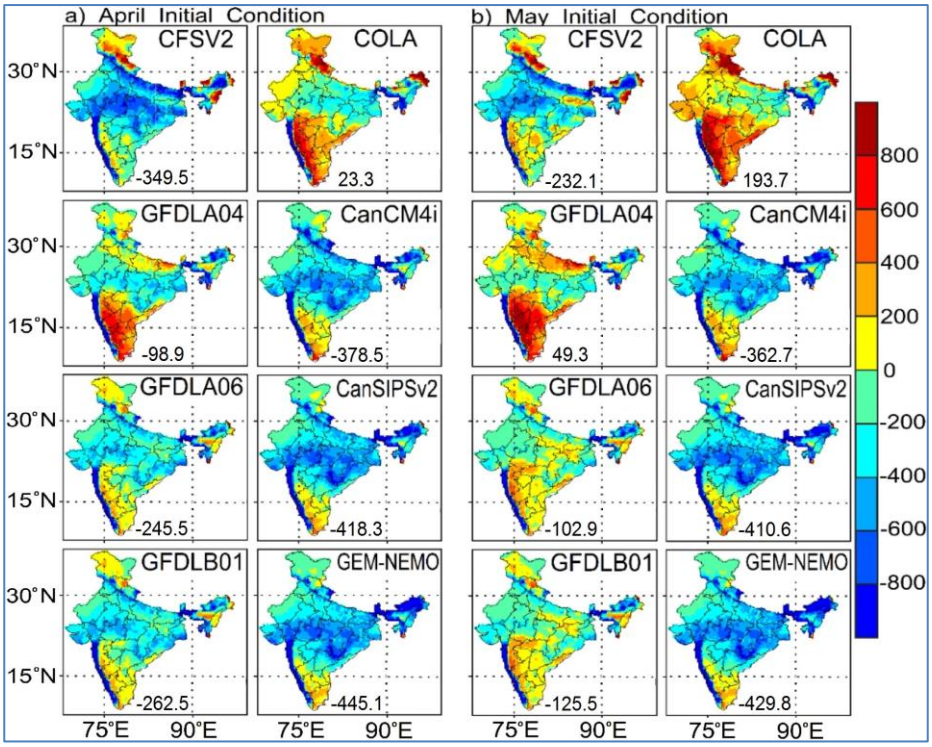


**Figs. 5(a&b).** Spatial distribution of bias error from the observed IMD for precipitation (mm) during the summer monsoon season for the period 1982-2019: a) April initial condition and b) May initial condition

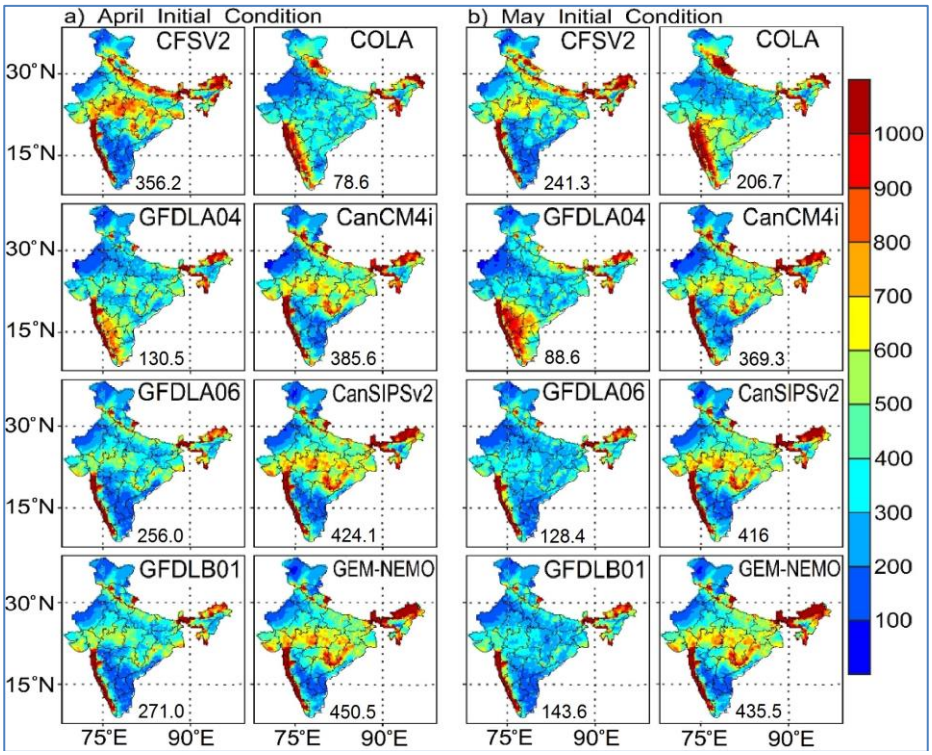


**Figs. 6(a&b).** Spatial distribution of RMSE from the observed IMD for precipitation (mm) during the summer monsoon season for the period 1982-2019: a) April initial condition and b) May initial condition

complicated topography, the WGs region of India has very intense rainfall of about 4000 mm during the summer monsoon season (Houze, 2012; Das *et al*., 2017). The GCMs are given a coarse resolution and are unable to calculate the orographic precipitation of the WGs. Over WGs, the GCMs underestimated the summer monsoon season by roughly 60-80%. For the period of JJAS 1982-2019 over the Indian subcontinent, Fig. 6 shows the spatial distribution of the root-mean-square errors (RMSE), which is a useful indicator of the bias and relationship between the simulation and observation. The RMSE is a measurement of a model's error based on quantitative forecasting data that shows how concentrated the model data are along the line of observational best fit (Stanski *et al*., 1989). For the April and May ICs, the central Indian plains, the foothills of the Himalayas, and WGs had the greatest geographical distribution of RMSE precipitation. Comparing the May ICs to the April ICs, the May ICs had slightly less RMSE precipitation. In CFSv2, GFDLA06, GFDLB01, CanCM4i, CanSIPSv2, and GEN-NEMO, the RMSE of the simulated precipitation was greater.

### 3.3. *Performance skill of GCM precipitation*

The correlation coefficient which is used to measure the prediction skill of the forecast for mean JJAS, 1982-2019 is presented in Fig. 7. The prediction skills were well captured in the simulated GCM precipitation over most of the regions for both ICs. The CC value increased all the simulated GCM precipitation from April to May ICs. Most of the simulated GCM precipitation has poor predictability over the Western Himalayas, parts of central India and NEI for both ICs. The simulated GCM JJAS precipitation had CCs above 0.5 in CFSv2, GFDLB01, CanSIPSv2, and GEN-NEMO with April ICs and in CFSv2, GFDLA04, GFDLA06, GFDLB01, CanCM4i, CanSIPSv2, and GEN-NEMO with May ICs.

The phase coherency index was calculated based on the direction of the anomaly index of each model and has a more suitable idea of the performance skills of a particular model. The phase coherency index was calculated in the same direction as the positive/negative anomalies of the models with observations. Fig.8 represents the spatial distribution of the phase coherency index of individual GCM models with both ICs. The spatial distribution of the phase coherency index was the highest over most regions above 0.5 with both ICs. The highest phase coherency index can be seen in NWI, central India and PI in GFDLA06, GFDLB01, CanCM4i, CanSIPSv2, and GEN-NEMO with April ICs and in CFSv2, GFDLA06, GFDLB01, CanCM4i, CanSIPSv2, and GEN-NEMO with May ICs. The slightly increased phase coherency index was found in most of the regions from April to May ICs, simulating GCM precipitation. COLA has a high phase coherency index from May to April ICs.

Fig. 9 presents a statistical summary of the correlation coefficients, normalized standard deviation, and mean percentage biases of the eight GCMs with IMD precipitation for April and May ICs obtained using the Taylor diagrams (Taylor, 2001) to assess the performance of each GCM model. Every GCM model exhibits a positive association and an increase in ICs from April to May. For April ICs, the highest CCs are CFSv2 and GFDLB01, whereas for May ICs, the greatest CCs are CFSv2, GFDLA04, GFDLB01, and CanSIPSv2. The IMD with the May to April ICs is much closer than the GCM normalized standard deviation. In comparison to the five GCM models that were output with May ICs, the normalized standard deviation for the seven GCM models ranges from 0.4 to 0.6.

GFDLA04, GFDLA06, and GFDLB01 have increased normalized standard deviations from April to May ICs. Except for COLA for April ICs and COLA and & GFDLA04 for May ICs, most GCM models show negative IMD biases. For the April to May ICs, the mean percentage biases decreased in the majority of the GCM models.

### 3.4. *Real-time predicted ERFS forecast and its verification.*

The percentage departures from long-period average (LPA) precipitation are displayed in the IMD and ERFS deterministic forecasts with April and May ICs during the summer monsoons of 2020 and 2021, as shown in Fig.10. The summer monsoon precipitation received 109% and 99% of its LPA for 2020 and 2021, respectively, over India. In the summer monsoon of 2020, most of the MSD had excess/normal precipitation except for Nagaland-Manipur-Mizoram-Tripura from the northeast region and western U.P., Uttarakhand, Himachal Pradesh, and J&K from the northern regions. During JJAS 2020, 14, 15 and 5 MSDs received excess, normal and deficient precipitation, respectively, out of 34 MSDs. JJAS 2021 had below-normal precipitation, and most of the MSD received normal precipitation of 21 MSD out of 34 MSD over central India and south peninsular India. Most excess precipitation during JJAS 2021 was received in 9 MSD out of 34 MSD over the west NWI and north PI, while deficient precipitation was received in 5 MSD out of 34 MSD over the NEI and northern regions of west UP and J&K. The ERFS deterministic precipitation forecast over India predicted 107% and 112% during JJAS 2020 and predicted 105% and 102% during JJAS 2021 with April and May ICs, respectively. The spatial distribution of

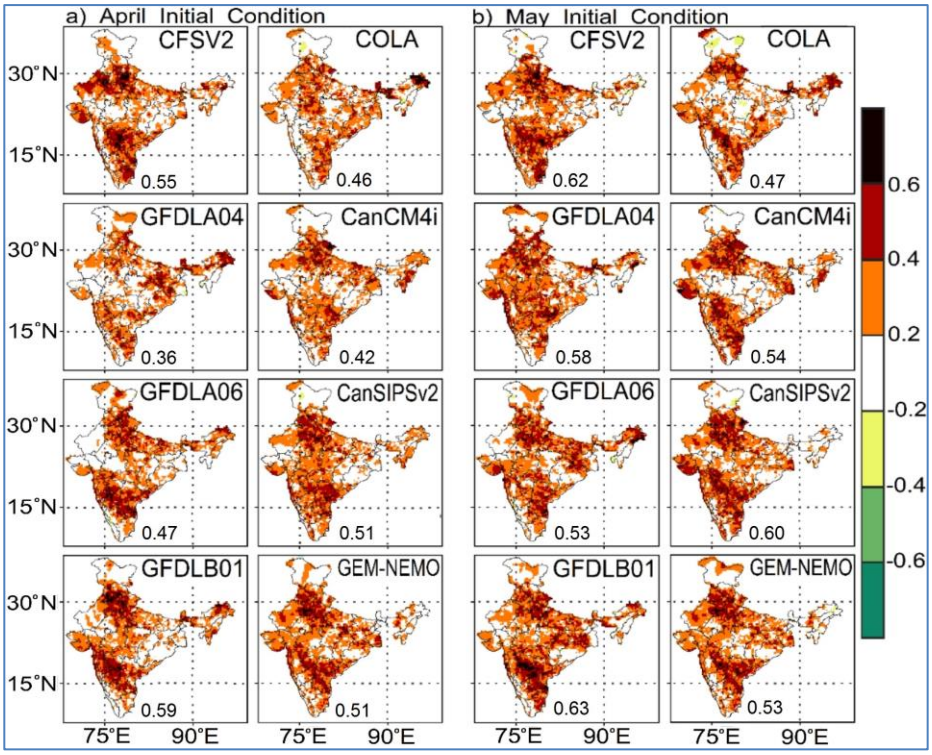


**Figs. 7(a&b).** Spatial distribution of temporal correlation coefficients between observed IMD for precipitation (mm) during the summer monsoon season for the period 1982-2019: a) April initial condition and b) May initial condition

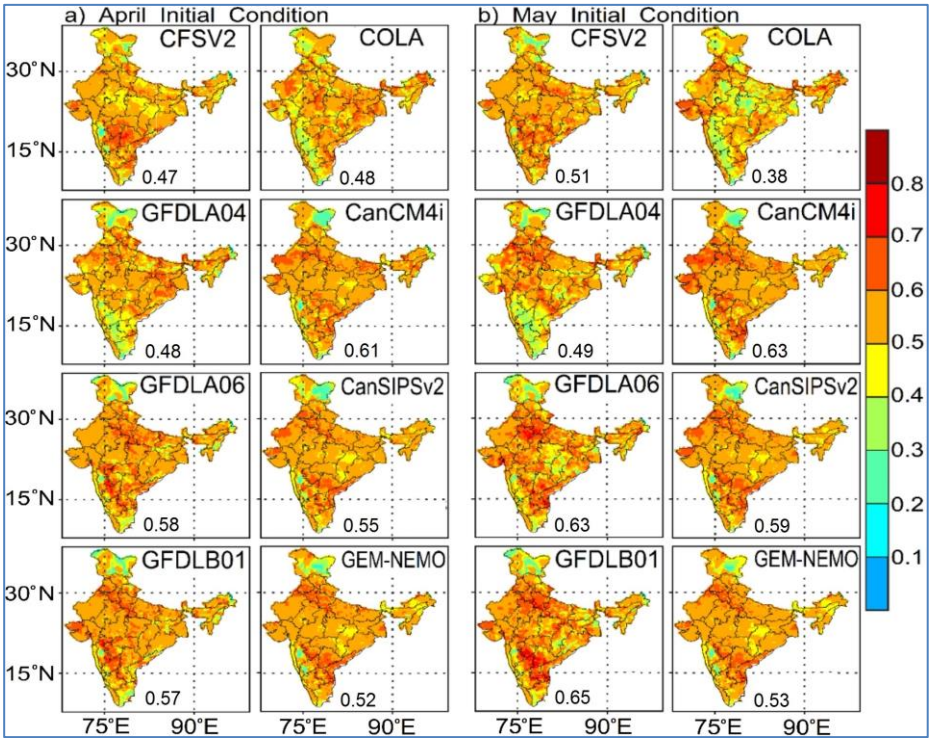


**Figs. 8(a&b).** Spatial distribution of the phase coherency of the individual GCM standardized precipitation anomaly index and IMD observed dataset during the summer monsoon season for the period from 1982 to 2019: a) April initial condition and b) May initial condition

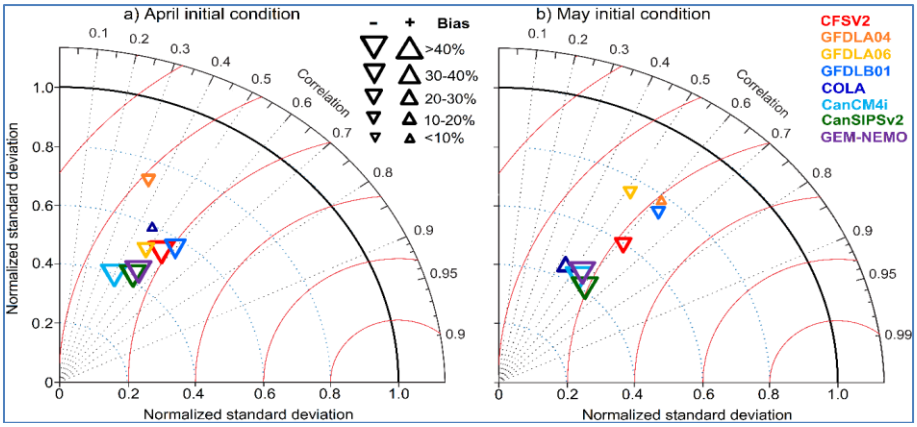


**Figs. 9(a&b)** Taylor diagrams exhibiting the correlation coefficients, normalized standard deviations and mean percentage biases of the eight GCM simulations and observed (IMD) precipitation during the summer monsoon season for the period 1982-2019: a) April initial condition and b) May initial condition. The mean percentage bias is positive in the upwards triangle and negative in the downwards triangle.

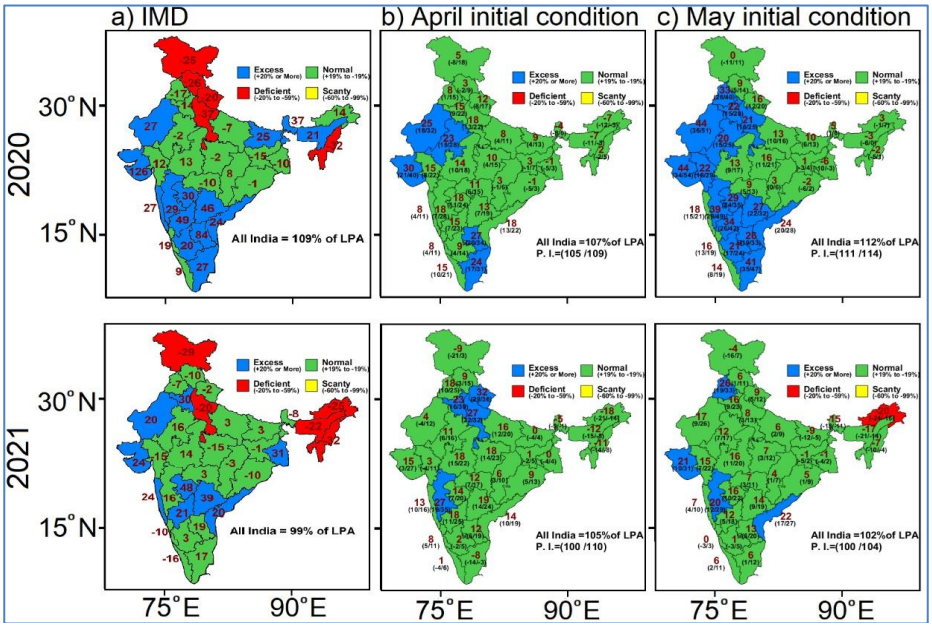


**Figs. 10(a-c).** Percentage departure precipitation of the long period average (LPA) of the actual (IMD) and ERFS deterministic forecasts during the summer monsoon season over the 34 meteorological subdivisions and over all of India: a) IMD, b) April initial condition and c) May initial condition obtained for 2020 (top row) and 2021 (bottom row). The four precipitation categories are recognized based on the percentage departure of LPA, viz. excess [20% or more], normal [-19% to 19%], deficit [-59% to -20%] and scanty [-60% or more]

precipitation from the LPA is a well-predicted ERFS forecast from the IMD for both summer monsoon seasons with both ICs. The ERFS forecast was well captured where it has received excess/normal precipitation. The ERFS forecast was poorly captured in the regions that have deficient precipitation. May ICs have more captured ERFS forecasts than April ICs during the summer monsoon seasons of 2020 and 2021.

The deterministic precipitation forecast was obtained using a 3×3 contingency table (Table 2) and has a measure of the skill score (Table 4) that verifies the precipitation forecast of a forecast and actual observation. The ERFS precipitation forecast has high ACCs of 0.53 and 0.59 for JJAS 2020, and 0.44 and 0.62 for JJAS 2021 with April and May ICs, respectively. The highest ACC was seen in May ICs compared with April ICs. The JJAS ERFS

**TABLE 4**

**Verification of the ERFS for monsoons in 2020 and 2021 starting in April and May**

| | | ACC | BIAS | POD | FAR | CSI | SR | MR | Forecast Error |
|---|---|---|---|---|---|---|---|---|---|
| 2020 | April | 0.53 | 0.79 | 0.62 | 0.22 | 0.53 | 0.78 | 0.38 | -2% |
| | May | 0.59 | 0.86 | 0.69 | 0.20 | 0.59 | 0.80 | 0.31 | 3% |
| 2021 | April | 0.44 | 0.69 | 0.52 | 0.25 | 0.44 | 0.75 | 0.48 | -6% |
| | May | 0.62 | 0.83 | 0.69 | 0.17 | 0.61 | 0.83 | 0.31 | -3% |

precipitation forecast underpredicted the BIAS skill at the MSD for the 2020 and 2021 seasons. The forecast errors (actual minus forecast divided by actual) are -2% and 3% during JJAS 2020 and -6% and -3% during JJAS 2021 with April and May ICs, respectively. The POD had a value of 0.69 for JJAS 2020 and 2021 with May ICs, while the lowest POD was 0.44 for JJAS 2021 with April ICs. The FAR values were lowest, ranging from 0.17 to 0.25 for both summer monsoon seasons with April and May ICs. The SR skill score is very high, ranging from 0.75 to 0.83 during JJAS 2020 and 2021 with both ICs. The MR skill score lies between 0.31 to 0.48, and a high MR score was found in the April ICs compared to the May ICs.

## 4. Conclusions

We evaluated eight GCMs to simulate precipitation for the inter comparison and performance over India during the summer monsoon season of 1982-2019. These results identified the multimodel ensemble models, that can predict Indian summer monsoon precipitation. These multimodel ensemble prediction models are used to generate real-time ERFS forecasts at 34 meteorological subdivisions of India for the summer monsoon seasons of 2020 and 2021 with April and May initial conditions. The real-time ERFS generation forecast was verified by the 3x3 contingency table used as a measure of the forecast skill score. The performances of CFSv2, GFDLA04, GFDLA06, GFDLB01, COLA, CanCM4i, CanSIPv2, and GEN-NEMO (eight GCM models) were evaluated with ICs of April and May over India for a 38-year period. The climatological pattern of JJAS precipitation was well captured in CFSv2, GFDLA06, GFDLB01, and COLA for April and May ICs, while all three Canadian models of CanCM4i, CanSIPv2, and GEN-NEMO were not captured. The intensities of the GCM-simulated precipitation were smaller than the observations (IMD), except for the COLA; however, the pattern precipitation intensity increased from April to May ICs. However, all the Canadian models did not capture the distribution pattern of the standard deviation well with both ICs. The standardized anomaly index was in close agreement with the CFSv2, GFDLA06, GFDLB01, CanSIPv2, and GEN-NEMO with observations with ICs of April and May. The spatial distribution of forecast error was underpredicted in the WGs, central India, and NEI, whereas it was overpredicted in southern India, as found in the majority of GCM models.

The root-mean-square errors were maximum over the mountainous regions and central India, where RMSE was reduced from April to May ICs in most of the GCMs. The RMSE simulated precipitation was maximum in CFSv2, GFDLA06, GFDLB01, CanCM4i, CanSIPSv2, and GEN-NEMO with ICs of April and May. The correlation coefficients and phase coherency index were the best skills in CFSv2, GFDLB01, CanSIPSv2, CanCM4i, and GEN-NEMO over most of the regions for both ICs.

The JJAS real-time ERFS deterministic precipitation prediction over India predicted 107% (April ICs) and 112% (May ICs), while IMD predicted 109% of its LPA for 2020. For JJAS 2021, the ERFS precipitation prediction has 105% (April ICs) and 102% (May ICs) while IMD has 99% of its LPA. The real-time ERFS forecast has been well predicted, spatially in most of the MSDs for both summer monsoon seasons with ICs of April and May. The ERFS forecast is well predicted for excess/normal intensity but poorly predicted for deficit intensity. The verification of the ERFS forecast obtained by the 3×3 contingency table has high accuracy for May ICs compared to April conditions. The ERFS forecast underpredicted the BIAS skill at the MSD. However, the forecast error over India was like the actual precipitation. The POD and SR skill scores were high, while the FAR and MR skill scores were low for May ICs compared to April ICs.

*Authors' Contributions*

Lata Vishnoi: Contributed to the conceptualization, methodology development, data analysis, and drafting of the manuscript.

R.S.K. Maurya: Contributed to data processing, model implementation, analysis and preparation of manuscript content. (*email- dk.maurya@imd.gov.in*)
D.R. Pattanaik: Provided scientific guidance and critically reviewed the manuscript. (*email-dr.pattanaik@imd.gov.in*)
Anupam Kumar: Supported data preparation and provided technical inputs.
K.K. Singh: Contributed agrometeorological insights and participated in manuscript review. (*email-kksingh2022@gmail.com)*
S.C. Bhan: Supervised the work and provided final critical evaluation. (*email - scbhanmet@yahoo.com*)
Priyanka Singh: Assisted with literature compilation and editorial support. (*email- cpriyanka04@gmail.com*).

*Disclaimer*: The contents and views presented in this research article/paper are the views of the authors and do not necessarily reflect the views of the organizations they belong to.

**References**


Abbe, C. 1901, "The physical basis of long-range weather forecasts", *Mon. Weath. Rev*., **29**, 551–561.

Acharya N., Chattopadhyay S., Mohanty U.C., Dash S.K. and Sahoo L.N. 2012, "On the bias correction of general circulation model output for Indian summer monsoon", *Meteorol Appl*, **20**, 349–356.

Acharya, N., Chattopadhyay, S., Mohanty, U.C. and Ghosh, K. 2014, "Prediction of Indian summer monsoon rainfall: a weighted multi-model ensemble to enhance probabilistic forecast skills", *Meteorological Applications*, **21**, 3, 724-732.

Agnew C. and Chappel, A., 1999, "Drought in the Sahel", *Geo. Journal*, **48**, 4, 299–311.

Ashok, K., Guan, Z., Saji, N. H. and Yamagata, T., 2004, "Individual and combined influences of ENSO and the Indian Ocean dipole on the Indian summer monsoon", *J. Clim*., **17**, 3141– 3155.

Barnston A.G. and Smith T.M., 1996, "Specification and prediction of global surface temperature and precipitation from global SST using CCA", *J. Clim.*, **9**, 2660–2697.

Berner, J., Doblas-Reyes, F.J., Palmer, T.N., Shutts, G. and Weisheimer, A., 2008, "Impact of a quasi-stochastic cellular automaton backscatter scheme on the systematic error and seasonal prediction skill of a global climate model", Philos. Trans. *Roy. Soc. London*, A366, 2561–2579.

Bewket, W. and Conway, D. 2007, "A note on the temporal and spatial variability of rainfall in the drought-prone Amhara region of Ethiopia", *Int. J. Climatol*, **27**, 1467 – 1477.

Brier, G.W. and Allen, R. A. 1951, "Verification of weather forecasts. Compendium of Meteorology, Boston", *American Meteorology Society*, 841-848.

Chaudhari, H.S., Pokhrel, S., Saha, S.K., Dhakate, A., Yadav, R.K., Salunke, K., Mahapatra, S., Sabeerali, C.T. and Rao, S.A. 2013, "Model biases in long coupled runs of NCEP CFS in the context of Indian summer monsoon", *Int. J. Climatol*., **33**, 1057–1069.

Cote, J., Gravel, S., Méthot, A., Patoine, A., Roch, M. and Staniforth, A. 1998, "The operational CMC-MRB Global Environmental Multiscale (GEM) model: Part I-Design considerations and formulation", *Mon. Wea. Rev*., **126**, 1373–1395.

Das, S., 2017, "Performance of region-of-influence approach of frequency analysis of extreme rainfall in monsoon climate conditions", *Int, J. Climatology*, **37**, 612-623.

Derome, J., Brunet, G., Plante, A., Gagnon, N., Boer, G.J., Zwiers, F.W., Lambert, S. and Ritchie, H., 2001, "Seasonal predictions based on two dynamical models", *Atmos.–Ocean*, **39**, 485–501.

Doblas-Reyes F.J., Deque, M. and Piedelievre, J.P., 2000, "Multi-model spread and probabilistic seasonal forecasts in PROVOST", *Q. J. R. Meteorol. Soc*. **126**, 2069–2088.

Doblas-Reyes, F.J., Hagedorn, R. and Palmer, T.N., 2005, "The rationale behind the success of multi-model ensembles in seasonal forecasting-II. Calibration and combination", *Tellus*, 57A, 234–252.

Edwards, D.C. and McKee, T.B., 1997, "Characteristics of 20th Century Drought in the United States at Multiple Times Scales", *Atmospheric Science Paper*, **634**, 1-30.

Fekedulegn, B.D., Colbert, J.J., Hicks, R.R. and Schuckers, M.E., 2002, "Coping with multicollinearity: an example on application of principal components regression in dendroecology", Newton Square, PA, Department of Agriculture, Forest Service, Northeastern Research Station.

Fowler, T. L., Jensen, T. L. and Brown, B. G., 2012, "Introduction to forecast verification. University Corporation for Atmospheric Research", 81 pp.

Gadgil, S. and Sajani, S., 1998, "Monsoon precipitation in the AMIP runs", *Clim. Dyn*., **14**, 659-689.

Gadgil, S. and Srinivasan, J., 2011, "Seasonal prediction of the Indian monsoon", *Curr. Sci*., 1003, 343-353.

Hagedorn, R., Doblas-Reyes, F.J. and Palmer, T.N., 2005, "The rationale behind the success of multimodel ensembles in seasonal forecasting-I", *Basic concept. Tellus*, 57A, 219–233.

Houze, R.A., 2012, "Orographic effects on precipitating clouds Rev" *Geophys*., **50**, 1-47.

Johnson, S.J., Turner, A. and Woolnough, S., 2017, "An assessment of Indian monsoon seasonal forecasts and mechanisms underlying monsoon interannual variability in the Met Office GloSea5-GC2 system", *Clim. Dyn*., **48**, 1447–1465.

Kar, S.C., Acharya, N., Mohanty, U.C. and Kulkarni, M.A. 2011, "Skill of monthly rainfall forecasts over India using multi-model ensemble schemes", *Int. J. Climatol*., **32**, 1271–1286.

Kharin, V. V., Teng, Q., Zwiers, F. W., Boer, G. J., Derome, J. and Fontecilla, J. S., 2009, "Skill assessment of seasonal hindcasts from the Canadian Historical Forecast Project", *Atmosphere-ocean*, **47**, 3, 204-223.

Kharin, V.V. and Zwiers, F.W., 2003, "Improved seasonal probability forecasts", *Journal of Climate*, **16**, 1684-1701.

Kharin, V.V. and Zwiers, F.W., 2002, "Climate predictions with multi-model ensembles", *J. Climate*, **15**, 793-799.

Kirtman, B.P. 2003, "The COLA anomaly coupled model: ensemble ENSO prediction", *Mon. Weather. Rev*., **131**, 2324-2341.

Kirtman, B.P. and Min, D., 2009, "Multimodel ensemble ENSO prediction with CCSM and CFS", *Monthly Weather Review*, **137**, 2908-2930.

Kirtman, B.P., Min, D, Infanti, J.M., Kinter, J.L., Paolino, D.A., Zhang, Q., Dool, H.V.D., Saha, S., Mendez, M.P., Becker, E., Peng, P., Tripp, P., Huang, J., DeWitt, D.G., Tippett, M.K., Barnston, A.G., Li, S., Rosati, A., Schubert, S.D., Rienecker, M., Suarez, M., Li, Z.E., Marshak, J., Lim, Y.K., Tribbia, J., Pegion, K., Merryfield, W.J., Denis, B. and Wood, E.F., 2014, "The North American multimodel ensemble: phase-1 seasonal-to-interannual prediction; phase-2 toward developing intraseasonal prediction", *Bull. Am. Meteor. Soc*., **95**, 585-601.

Koteswaram, P. and Rao, N.B., 1963, "Formation and Structure of Indian Summer Monsoon Depressions", *Australian Meteorological Magazine*, **41**, 2-75.

Kripalani, R.H., Kulkarni, A., Sabade, S.S. and Khandekar, M.L., 2003, "Indian monsoon variability in a global warming scenario", *Nat. Hazards*, **29**, 189-206.

Krishnamurti, T.N., Kishtawal, C.M., Shin, D.W. and Williford, C.E. 2000a, "Improving tropical precipitation forecasts from a multi-analysis superensemble", *Journal of Climate*, **13**, 4217-4227.

Krishnamurti, T.N., Kishtawal, C.M., Shin, D.W. and Williford, C.E. 2000b, "Multi-model super ensemble forecasts for weather and seasonal climate", *Journal of Climate*, **13**, 4196-4216.

Krishnamurti, T.N., Thomas, A., Simon, A. and Kumar, V., 2010, "Desert air incursions, an overlooked aspect, for the dry spells of the Indian summer monsoon", *J. Atmos. Sci*., **67**, 3423–3441.

Meehl, G., Washington, A. and Warren, M., 1993, "South Asian summer monsoon variability in a model with doubled atmospheric carbon dioxide concentration", *Science*, **260**, 1101-1104.

Merryfield, W.J., Lee, W.S., Boer, G.J., Kharin, V.V., Scinocca, J.F., Flato, G.M., Ajay Mohan, R.S., Fyfe, J.C., Tang, Y. and Polavarapu, S. 2013, "The Canadian Seasonal to Interannual Prediction System. Part I: Models and initialization", *Mon. Wea. Rev*., **141**, 2910–2945.

Mohanty, M., Sinha, P., Maurya, R. and Mohanty, U.C., 2018, "Moisture flux adjustments in RegCM4 for improved simulation of Indian summer monsoon precipitation", *Clim. Dyn*., **52**, 7049-7069.

Mohanty, U.C., Nageswararao, M.M., Sinha, M., Nair, A., Singh, A., Rai, R.K., Kar, S.C., Ramesh, K.J., Singh, K.K., Ghosh, K., Rathore, L.S., Sharma, R., Kumar, A., Dhekale, B.S., Maurya, R.K.S., Sahoo, R.K., Dash, G.P., 2019a' "Evaluation of performance of seasonal precipitation prediction at regional scale over India". *Theor Appl Climatol* **135**, 3-4, 1123–1142. https://doi.org/10.1007/s00704-018-2421-9.

Mohanty, U.C., Sinha, P., Mohanty, M.R., Maurya, R.K.S., Rao, M.M.N. and Pattanaik, D.R. 2019b, "A review on the monthly and seasonal forecast of the Indian summer monsoon". *Mausam*. **70**, 3, 425–442.

Murphy, A.H. and Winkler, R.L., 1992, "Diagnostic verification of probability forecasts", *International Journal of Forecasting*, **7**, 435-455.

Murphy, A. H., Brown, B.G. and Chen, Y. S. 1989, "Diagnostic verification of temperature forecast", *Wea. & Forecasting*, **4**, 485-501.

Nageswararao, M.M., Mohanty, U.C., Osuri, K.K. and Ramakrishna, S.S.V.S. 2016. Prediction of winter precipitation over northwest India using ocean heat fluxes, *Clim. Dyn*., **47**, 7, 2253–2271.

Nair, A., Mohanty, U. C. and Panda, T. C. 2015, "Improving the performance of precipitation outputs from Global Climate Models to predict monthly and seasonal rainfall over the Indian subcontinent", *Comptes Rendus Geoscience*, **347**, 2, 53-63.

Nair, A., Mohanty, U.C. and Acharya, N., 2012, "Monthly prediction of rainfall over India and its homogeneous zone: a supervised principal component regression approach on global climate models", *Theor. Appl. Climatol*., **111**, 327-339.

Niyogi, D., Kishtawal, C., Tripathi, S. and Govindaraju, R.S. 2010, "Observational evidence that agricultural intensifcation and land use change may be reducing the Indian summer monsoon rainfall", *Water Res Res*., **46**, 3, 1-17.

Pai, D., Sridhar, S., Badwaik, L. and Rajeevan, M.R., 2014, "Development of a new high spatial resolution (0.250 × 0.250) Long period (1901–2010) daily gridded rainfall data set over India and its comparison with existing datasets over the region". *Mausam*, **1**, 1–18.

Palmer, T. N., Doblas-Reyes, F.J., Weisheimer, A. and Rodwell, M.J. 2008, "Toward seamless prediction calibration of climate change projections using seasonal forecasts", *Bull. Amer. Meteor. Soc*., **89**, 459-470.

Palmer, T.N., Alessandri, A., Andersen, U., Cantelaube, P. and Davey, M. 2004, "Development of a European multi-model ensemble system for seasonal to interannual prediction (DEMETER)", *Bull. Am. Meteorol. Soc*., **85**, 853-872.

Parthasarathy, B., Munot, A.A. and Kothawale, D.R. 1994, "All-India monthly and seasonal rainfall series: 1871–1993", *Theor. Appl. Climatol*., **49**, 217–224.

Pattanaik D. R. and Kumar, A., 2010, "Prediction of summer monsoon rainfall over India using the NCEP climate forecast system", *Clim. Dyn*. **34**, 557–572.

Pavan, V. and Doblas-Reyes, F. J., 2000, "Multi-model seasonal hindcasts over the Euro-Atlantic: Skill scores and dynamic features", *Climate Dyn*, **16**, 611–625.

Pegion, K., and Sardeshmukh, P. D. 2011, "Prospects for Improving Subseasonal Predictions", *Mon. Wea. Rev*., **139**, 3648–3666.

Peng, P., Kumar, A., Dool, H.V.D. and Barnston, A.G. 2002, "An analysis of multimodel ensemble predictions for seasonal climate anomalies", *J. Geophys. Res*., **107**, 4710.

Phillips, N.A. 1956, "The general circulation of the atmosphere: A numerical experiment", *Quarterly Journal of the Royal Meteorological Society*, **82**, 123-164.

Pillai, P.A., Rao, S.A. and Srivastava, A. 2021, "Impact of the tropical Pacific SST biases on the simulation and prediction of Indian summer monsoon rainfall in CFSv2, ECMWF-System4, and NMME models", *Clim. Dyn*., **56**,1699-1715.

Pillai, P.A., Rao, S.A., Dandi, R.A., Pradhan, M. and George, G., 2018, "Seasonal prediction skill of Indian summer monsoon rainfall in NMME models and monsoon mission CFSv2", *Int. J. Climatol*., **38**, 847–861.

Rajeevan M. and Nanjundiah, R.S., 2009, "Coupled model simulations of twentieth century climate of the Indian summer monsoon", *Curr. Trends Sci*. 537–567.

Richardson, L.F. 1922, "Weather Prediction by Numerical Process", Cambridge University Press .2nd Edn. with Foreward by Peter Lynch.

Ritchie, H., 1991, "Application of the semi-Lagrangian method to a multilevel spectral primitive-equation model", *Quart. J. Roy. Meteor. Soc*., **117**, 91–106.

Sabeerali, C.T., Dandi, R.A., Dhakate, A., Salunke, K., Mahapatra, S. and Rao, S.A., 2013, "Simulation of boreal summer intra-seasonal oscillations in the latest CMIP5 coupled GCMs", *J Geophys Res Atmospheres*, **118**, 4401–4420.

Saha, S., Moorthi, S., Wu, X., Wang, J., Nadiga, S., Tripp, P., Behringer, D., Hou, Y.T., Chuang, H.Y., Iredell, M., Ek, M., Meng, J., Yang, R., Mendez, M.P., Dool, H, Zhang, Q., Wang, W. Chen, M. and Becker, E. 2014, "The NCEP Climate Forecast System version 2", *J. of Climate*, **27**, 2185–2208.

Saji, N.H., Goswami, B.N., Vinayachandran, P.N. and Yamagata, T. 1999, A dipole mode in the tropical Indian Ocean, *Nature*, **401**, 360– 363.

Scinocca, J.F., McFarlane, N.A., Lazare, M. and Li, J. 2008, "The CCCma third generation AGCM and its extension into the middle atmosphere", *Atmos. Chem. Phys.*, **8**, 7055–7074.

Simmons, A.J. and Hollingsworth, A. 2002, "Some aspects of the improvement in skill of numerical weather prediction", *Quart. J. Roy. Meteor. Soc*.**, 128**, 647–677.

Sinha, P., Mohanty, U.C., Kar, S.C., Dash, S.K., Robertson, A. and Tippett, M. 2013, "Seasonal prediction of the Indian summer monsoon rainfall using canonical correlation analysis of the NCMRWF global model products", *Int. J. Climatol*., **33**, 1601–1614.

Slingo, J. and Annamalai, H. 2000, "The El Nino of the century and the response of the Indian summer monsoon", *Mon. Wea. Rev*., **128**, 1778–1797.

Smagorinsky, J. 1963, "General Circulation Experiments with the Primitive Equations", 99–164.

Smith, G. C., Belanger, J.M., Roy, F., Pellerin, P., Ritchie, H., Onu, K., Roch, M., Zadra, A., Colan, D.C., Winter, B., Fontecilla, J.S. and Deacu, D., 2018, "Impact of coupling with an ice-ocean model on global medium-range NWP forecast skill", *Mon. Wea. Rev*., **146**, 1157–1180.

Smith, G., Davidson, C.F. and Lu, Y., 2013, "The CONCEPTS initiative: Canadian operational network of coupled environmental prediction systems", *J. Ocean Technol*., **8**, 80–81.

Sperber, K.R., Annamalai, H., Kang, L.S., Kitoh, A., Moise, A., Turner, A., Wang, B., Zhou, T., 2012, "The Asian summer monsoon: an intercomparison of CMIP5 vs. CMIP3 simulations of the late 20th century", *Clim. Dyn*., **41**, 2711–2744.

Stanski, H.R., Wilson, L.J. and Burrows, W.R., 1989, "Survey of common verification methods in meteorology", World Weather Watch Tech. Rept. No.8, WMO/TD No.358, WMO, Geneva, 114.

Stephenson, D. B. and Doblas-Reyes, F. J., 2000, "Statistical methods for interpreting Monte Carlo ensemble forecasts", *Tellus*, 52A, 300–322.

Taylor, K.E., 2001, "Summarizing multiple aspects of model performance in a single diagram", *J. Geophys. Res*., **106**, 7183–7192.

Tippett, M.K., Ranganathan, M., L'Heureux, M., Barnston, A.G., and DelSole, T., 2019, "Assessing probabilistic predictions of ENSO phase and intensity from the North American Multimodel Ensemble", *Climate Dynamics*, **53**, 12, 7497-7518.

Trenary, L., DelSole, T., Tippett, M.K. and Pegion, K., 2017, "A new method for determining the optimal lagged ensemble". *J. Adv. Modeling Earth Syst*., **9**, 1, 291–306.

Webster, P., Moore, A. and Loschnigg, J., 1999, "Coupled Ocean–atmosphere dynamics in the Indian Ocean during 1997–98", *Nature*, **401**, 356–360.

Wilks, D.S., 1995, "Statistical methods in the atmospheric sciences", Academic Press, San Diego.

Wilks, D.S., 2011, "Statistical Methods in the Atmospheric Sciences", Academic Press.

Yu, Z., Chu, P.S. and Schroeder, T., 1997, "Predictive skills of seasonal to annual rainfall variations in the U.S. Affiliated Pacific Islands: canonical correlation analysis and multivariate principal component regression approaches", *J, Clim*, **10**, 2586–2599.

Yun, W.T., Stefanova, L. and Krishnamurti, T.N., 2003, "Improvement of the super ensemble technique for seasonal forecasts", *Journal of Climate*, **16**, 3834-3840.

Yun, W.T., Stefanova, L., Mitra, A.K., Kumar, T.S.V.V., Dewar, W., and Krishnamurti, Y.N., 2005, "A multi-model super ensemble algorithm for seasonal climate prediction using DEMETER forecasts", *Tellus*, **57**, 3, 280-289.